

# Cadmium(II) Schiff base Complex Containing 5-Fluoroisatin Moiety: Synthesis, Characterization, Antibacterial Activity and Structural Studies

Mohd Abdul Fatah Abdul Manan<sup>1,\*</sup> and David Bradford Cordes<sup>2</sup>

<sup>1</sup>Faculty of Applied Sciences, Universiti Teknologi MARA, 40450, Shah Alam, Selangor, Malaysia

<sup>2</sup>EaStCHEM School of Chemistry, University of St Andrews, North Haugh, St Andrews, KY16 9ST, United Kingdom

(\*Corresponding author's e-mail: abdfatah@uitm.edu.my)

Received: 30 May 2021, Revised: 30 June 2021, Accepted: 7 July 2021

## Abstract

The Schiff base ligand, HSB5FISA (**H1**), obtained by the condensation of S-benzylthiocarbamate with 5-fluoroisatin, has been employed to synthesize a new cadmium(II) complex, Cd(SB5FISA)<sub>2</sub> (**2**) (SB5FISA = monoanionic form of **H1**). The complex has been characterized by elemental analysis, molar conductivity, magnetic susceptibility, inductively coupled plasma atomic emission spectroscopy (ICP-AES), Fourier-transform infrared spectroscopy (FT-IR) and ultraviolet-visible spectroscopy (UV-Vis). The crystallographic study of Cd(SB5FISA)<sub>2</sub>·2DMSO (**2a**) (DMSO = dimethyl sulfoxide) was conducted using single-crystal X-ray diffraction. The crystal structure of **2a** confirmed the presence of 6-coordinated cadmium in a distorted octahedral environment. Ligand **H1** behaves in a tridentate monoanionic fashion, coordinating to a cadmium(II) metal centre through the thiolate sulfur, azomethine nitrogen and carbonyl oxygen. The antibacterial activity of both **H1** and **2** was examined against 4 different bacterial strains using the disc diffusion method. Complex **2** showed significant inhibitory effect against *Bacillus subtilis* with an inhibition zone of 14 mm, comparable to the standard antibiotic streptomycin.

**Keywords:** Cadmium(II), Dithiocarbamate, 5-fluoroisatin, Single-crystal structure, Antibacterial

## Introduction

Carbon-fluorine bonds have an important role in biology, medicine and material sciences [1-4]. Currently, many marketed agrochemicals and pharmaceutical drugs contain at least 1 fluorine or trifluoromethyl group [5]. The introduction of a fluorinated substituent atom can affect the basicity, dipole moment, hydrogen bonding ability and binding affinity of organic molecules [6]. Another established effect of fluorination is that the substitution of hydrogen with fluorine leads to minimal steric changes to the host motifs. For example, fluoromuscimol was found to possess potent and selective effects on the extrasynaptic GABA<sub>A</sub> receptors ( $\alpha_4\beta_2\delta$ ) comparable to that of the parent muscimol [7]. Thus, fluorine acts as a bioisostere of hydrogen, and it has been widely employed in medicinal chemistry in this regard [8].

There has been a greater demand on versatile organic substances that can be utilized in the pharmaceutical industry. Schiff bases or imines are one of the most valuable organic compounds as they exhibit highly potential of applications in fundamental and applied science and have been extensively employed in organic synthesis to construct various molecular architectures [9,10]. Chemically, imines are obtained via the condensation reaction between aldehydes or ketones (including aliphatic, aromatic and heterocyclic) with various primary amines under specific conditions of temperature or pH [11]. Besides their ease of formation, this class of compounds have been applied in coordination chemistry due to their multiple coordination sites exhibiting interesting coordination modes towards various metals [12-16]. Imines derived from halogen-substituted isatins have been reported to display potential chemotherapeutic uses [17,18]. Among them, the 5-fluoro-substituted isatin dithiocarbamate Schiff base ligand is of interest owing to its ability to inhibit the proliferation of human breast cancer cell lines [18].

Although researchers have made great progress in developing novel synthetic strategy to construct metal complexes, limited studies are available in the literature to describe the synthesis and biological activities of dithiocarbamate complexes bearing 5-haloisatin moieties. Cadmium has been chosen in this

study due to its potent antibacterial activity against similar bacterial strains reported previously [16]. Taking into account the importance of both imine and fluorinated compounds in the medicinal chemistry, we have synthesized and structurally characterized a novel dithiocarbazate cadmium(II) complex with 5-fluoroisatin ligand. Biological study of this compound with emphasis on its possible application as a novel antibacterial agent is also reported.

## Materials and methods

All reagents and solvents were purchased from commercial sources (Sigma-Aldrich, Fluka and Merck) and used without purification. Melting points were determined with an Electrothermal IA9100 digital point apparatus and are uncorrected. Elemental analysis was performed on a LECO CHNS-932 elemental analyser (LECO, Saint Joseph, MI, USA). The determination of cadmium content presence in Cd(SB5FISA)<sub>2</sub> (**2**) was made using a Perkin-Elmer Plasma 1000 Emission Spectrometer. IR spectra were acquired on a Perkin-Elmer FT IR 1750X spectrophotometer (4000 - 400 cm<sup>-1</sup>) using the potassium bromide (KBr) pellet method. Conductivity was measured in DMSO using a Jenway 4310 conductivity meter fitted with a dip-type cell with a platinized electrode. Magnetic moment value of Cd(SB5FISA)<sub>2</sub> (**2**) was measured using a Sherwood Scientific MSB-AUTO magnetic susceptibility balance. UV-Vis spectra were recorded with a Shimadzu UV-2501 PC Recording Spectrophotometer in the 200 - 1000 nm region.

### Synthesis of HSB5FISA (H1)

HSB5FISA was synthesized following a previously reported literature procedure [18]. 5-Fluoroisatin (825 mg, 5 mmol) was dissolved in hot ethanol (95 %) (10 mL) then added gradually to an equimolar amount of S-benzylidithiocarbazate (990 mg, 5 mmol) dissolved in hot ethanol (95 %) (10 mL). The reaction mixture was heated at 80 °C, stirred for 20 min and allowed to stand at room temperature for 30 min. The resulting dark red solid was filtered, washed with cold ethanol, recrystallized from ethanol and dried under vacuum. Yield 1.40 g, 81 %. The melting point and spectroscopic data matched that in the literature [18]. UV-Vis [ $\lambda_{\text{max}}$ , DMSO, nm (Log  $\epsilon$  mol<sup>-1</sup> l cm<sup>-1</sup>): 262(4.12) and 380(4.35).

### Synthesis of Cd(SB5FISA)<sub>2</sub> (**2**)

A hot ethanolic solution (4 mL) of cadmium acetate dihydrate (67 mg, 0.25 mmol) was added slowly to a solution of **H1** (173 mg, 0.5 mmol) in 5 mL of hot ethanol (95 %). The reaction mixture was heated with constant stirring for 20 min. The resulting solution was concentrated and allowed to cool to room temperature. The resulting red precipitate was filtered, washed thoroughly with ethanol for 3 times (3×5 mL) and dried in vacuum over anhydrous silica gel to afford the pure complex. Yield 146 mg, 73 %. m.p 266 - 267 °C. Anal. Calc. for C<sub>32</sub>H<sub>22</sub>CdF<sub>2</sub>N<sub>6</sub>O<sub>2</sub>S<sub>4</sub> required: C, 47.97; H, 2.77; N, 10.49; S, 16.01; Cd, 14.03. Found: C, 47.42; H, 2.45; N, 10.45; S, 15.94; Cd, 13.85 %. Selected IR (KBr pellet, cm<sup>-1</sup>)  $\nu$ (C=O) 1680;  $\nu$ (C=N) 1584;  $\nu$ (N-N) 1050;  $\nu$ (C-S) 1000. UV-Vis [ $\lambda_{\text{max}}$ , DMSO, nm (Log  $\epsilon$  mol<sup>-1</sup> l cm<sup>-1</sup>)] 265(4.37), 416(4.38). Molar conductivity,  $\Lambda$  (DMSO, 10<sup>-3</sup> M,  $\Omega^{-1}$  cm<sup>2</sup> mol<sup>-1</sup>): 0.20.  $\mu_{\text{eff}}$  = Diamagnetic. Dark red X-ray quality crystals of Cd(SB5FISA)<sub>2</sub>·2DMSO (**2a**) were obtained from slow evaporation of a DMSO solution of **2**.

### Single crystal x-ray diffraction

X-ray diffraction data for compound **2a** were measured at 25 °C using a Bruker SMART 1000 CCD diffractometer with graphite monochromated Mo K $\alpha$  radiation ( $\lambda = 0.71073$  Å). The data collected were reduced and corrected for Lorentz and polarization using SAINT [19] and a multiscan absorption correction was applied using SADABS [20]. The structure was solved by direct methods (SIR 2011 [21]) and refined by full-matrix least-squares against F<sup>2</sup> (SHELXL-2018/3 [22]). All non-H atoms were refined anisotropically, and hydrogen atoms (except NH hydrogens) were refined using a riding model. The NH hydrogen atoms were located in the difference Fourier map and refined isotropically subject to a distance restraint. Both the DMSO molecules showed whole-molecule disorder and were refined over 2 sites (refined occupancies 0.76:0.24 and 0.65:0.35). The heteroatoms in the disordered solvent were refined anisotropically, but carbon atoms were refined isotropically, and distance restraints were applied. All calculations were performed using the Olex2 [23] interface. Deposition number **2085794** contains the supplementary crystallographic data for this paper. These data are provided free of charge by the joint Cambridge Crystallographic Data Centre and Fachinformationszentrum Karlsruhe Access Structures service [www.ccdc.cam.ac.uk/structures](http://www.ccdc.cam.ac.uk/structures).

Crystal data. C<sub>36</sub>H<sub>34</sub>CdF<sub>2</sub>N<sub>6</sub>O<sub>4</sub>S<sub>6</sub>,  $M = 957.45$ , triclinic,  $a = 11.684(4)$ ,  $b = 12.491(4)$ ,  $c = 16.275(5)$  Å,  $\alpha = 84.942(5)$ ,  $\beta = 72.788(5)$ ,  $\gamma = 65.979(4)$  °,  $V = 2071.2(11)$  Å<sup>3</sup>,  $T = 298$  K, space group  $P\bar{1}$  (no. 2),

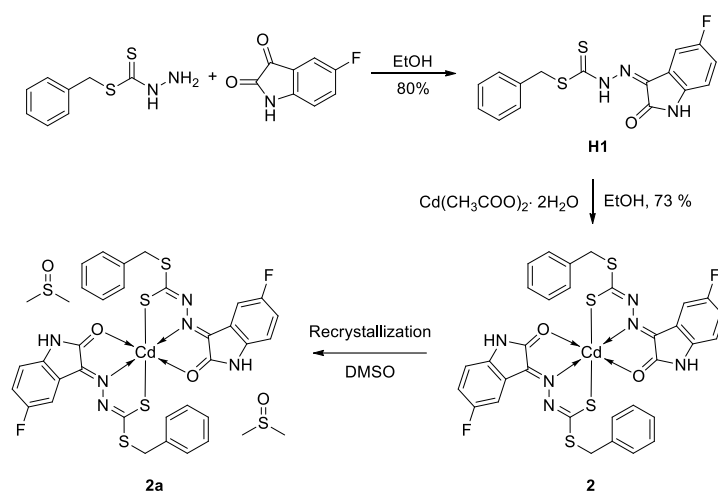
$Z = 2$ , 23522 reflections measured, 9456 unique ( $R_{\text{int}} = 0.0261$ ), which were used in all calculations. The final  $R_1 [I > 2\sigma(I)]$  was 0.0476 and  $wR_2$  (all data) was 0.1313.

### Qualitative antimicrobial assay

The biological activity of **H1** and its cadmium(II) complex **2** were assayed in vitro by measuring the inhibition zones (mm) against both Gram-positive (methicillin-resistant *Staphylococcus aureus* (MRSA), *Bacillus subtilis*) and Gram-negative bacteria (*Pseudomonas aeruginosa*, *Salmonella choleraesuis*) in order to assess their antibacterial potential. The bacterial cultures were prepared using the disc diffusion technique as previously described [24]. Briefly, a lawn of microorganisms was prepared by pipetting and evenly spreading inoculum ( $10^{-4}$  mL, adjusted turbidometrically to  $10^5$  -  $10^6$  cfu/mL (cfu: Colony forming units) onto nutrient agar set in Petri dishes. A sterilized filter paper discs (Whatman No. 1, 6 mm diameter) impregnated with a stock solution of each compound (100 mg/mL) in DMSO was allowed to dry before being transferred onto the inoculated agar plates and incubated at 37 °C for 24 h.

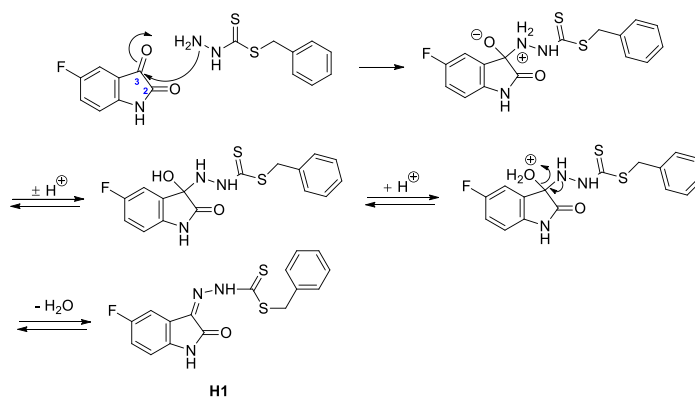
### Results and discussion

The synthetic route to Schiff base **H1** and its cadmium(II) complex,  $\text{Cd}(\text{SB5FISA})_2$  (**2**) is shown in **Scheme 1**. Recrystallization of **2** in DMSO afforded crystalline complex **2a**. The obtained crystals were non-hygroscopic and stable in air.



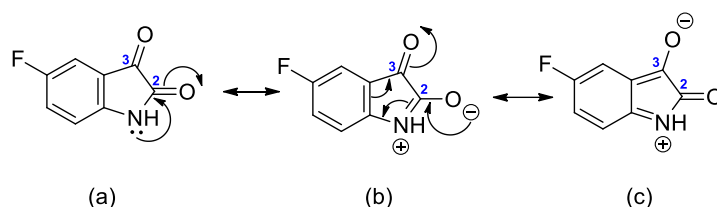
**Scheme 1** Synthesis of **H1** and complex **2**.

**Scheme 2** illustrates a proposed mechanism for **H1** formation. The first step involves nucleophilic attack by the lone pair of the  $\text{NH}_2$  of S-benzylthiocarbonylhydrazide on the 3-carbonyl of the 5-fluoroisatin moiety. Protonation of the hydroxy group of the carbinolamine intermediate furnishes a hydronium ion, thus converting it into a better leaving group. The last step of the mechanism involves displacement of a water molecule forming the desired Schiff base **H1**.



**Scheme 2** Proposed mechanism for **H1** formation.

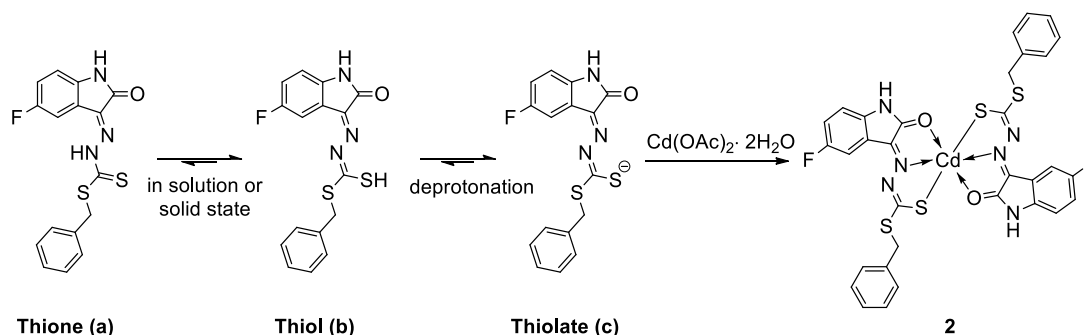
The 2 carbonyl groups in 5-fluoroisatin exhibit different reactivity toward nucleophilic reagents (**Scheme 3**). Due the presence of adjacent nitrogen atom, the 2-carbonyl has considerable amide character. Delocalization of the lone pair electrons onto the 2-carbonyl results in a reduction of its electrophilicity (**Scheme 3b**). Conjugation of the nitrogen with the 3-carbonyl is also possible (**Scheme 3c**), but this process leads to the disruption of the aromaticity of the benzene ring and thus is less favourable. It is therefore anticipated that the carbonyl at position 3 would be relatively more vulnerable toward nucleophiles, compared to the carbonyl at position 2. On this basis, selective substitution at C(3) should be possible.



**Scheme 3** Carbonyl reactivity of 5-fluoroisatin.

### Spectroscopic and Physical Characterization of Complex 2

The infrared spectrum of compound **H1** displayed a  $\nu(\text{C}=\text{S})$  band at  $1056\text{ cm}^{-1}$ . In addition, no  $\nu(\text{S}-\text{H})$  thiol signal was observed at  $\text{ca } 2750\text{ cm}^{-1}$ , suggesting that the thione form was the predominant species in the solid state (**Scheme 4a**). The characteristic bands of complex **2** differ from the free ligand and provide indications regarding to the coordination mode of ligand **H1**. The absence of the  $\text{C}=\text{S}$  signal followed by the formation of a new  $\nu(\text{C}-\text{S})$  peak at  $1000\text{ cm}^{-1}$  in the infrared spectrum of **2** confirmed that the conversion of thione to thiol form (**Scheme 4b**) had occurred during complexation. This indicates that in the present of cadmium(II) acetate in an ethanolic solution, the thione tautomer gets converted to the thiol form and coordinates to the metal centre via its deprotonated thiolate species (**Scheme 4c**) [20]. Bands attributed to  $\nu(\text{C}=\text{N})$ ,  $\nu(\text{C}=\text{O})$  and  $\nu(\text{N}-\text{N})$  showed a shift to lower wavenumber on formation of complex **2**, indicating coordination through the azomethine nitrogen and carbonyl oxygen [12].



**Scheme 4** Thione, thiol and thiolate form of Schiff base **H1** and the reaction with cadmium acetate dihydrate to form the cadmium(II) complex **2**.

The electronic spectra data of **H1** and **2** are tabulated in **Table 1**. **H1** exhibits 2 spectral bands at 262 and 380 nm, which can be assigned to the  $(\pi \rightarrow \pi^*)$  aromatic ring of the dithiocarbazate and 5-fluoroindole moiety, and  $(n \rightarrow \pi^*)$  of the carbonyl ( $\text{C}=\text{O}$ ), thione ( $\text{C}=\text{S}$ ) and azomethine ( $\text{C}=\text{N}$ ) groups respectively (**Table 1**) [12,25]. On the other hand, the spectrum of the cadmium complex showed only an intra-ligand transition with the  $n \rightarrow \pi^*$  band experiencing a shift to longer wavelength (265 nm). In addition, an intense band is observed at 416 nm corresponds to the  $\text{S} \rightarrow \text{M}^{\text{II}}$  ligand-to metal charge transfer (LMCT), which further confirms the coordination of the  $\text{Cd}(\text{II})$  ion via the thiolate sulfur atom [26]. No

d-d transition peak was observed since the Cd<sup>2+</sup> ion has a d<sup>10</sup> configuration. Complex **2** is diamagnetic and non-electrolyte as indicated by its low molar conductance value (0.2 Ω<sup>-1</sup> cm<sup>2</sup> mol<sup>-1</sup>).

**Table 1** UV-Vis spectral, molar conductance and magnetic moment data of **H1** and **2**.

Compound	UV-Vis spectra bands λ <sub>max</sub> , nm (Log ε, mol <sup>-1</sup> l cm <sup>-1</sup> )	Conductance Ω <sup>-1</sup> cm <sup>2</sup> mol <sup>-1</sup>	μ <sub>eff</sub> B.M
H1	262(4.12), 380(4.35)	-	-
2	265(4.37), 416(4.38)	0.2	Diamagnetic

### Structural analysis of complex **2a**

X-ray structural analysis shows that the Cd(II) complex crystallizes in the triclinic *P* $\bar{1}$  space group. **Figure 1** depicts the structure of six-coordinate complex **2a**. The asymmetric unit consists of a single cadmium complex with 2 DMSO solvent molecules. The central cadmium(II) adopts a distorted octahedral configuration with each ligand coordinating via its azomethine nitrogen [Cd-N, 2.319(3), 2.321(3)], thiolate sulfur [Cd-S, 2.553(12), 2.566(12)] and the carbonyl oxygen of the isatin moiety [Cd-O, 2.523(3), 2.539(2)], forming 5 membered chelate rings as bicyclic pairs. Each ligand's bicyclic chelate system were approximately planar, with maximum deviations from the mean-plane of 0.046 Å and 0.048 Å. The dihedral angle formed between these 2 mean planes was 81.80°, indicative of the distortion from an ideal octahedral geometry around the Cd(II) centre.

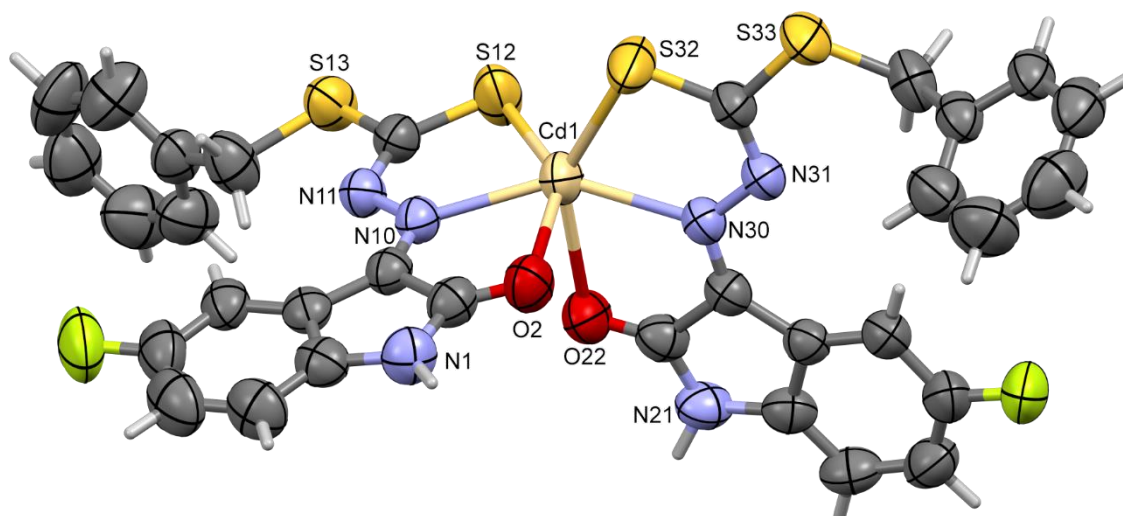


**Figure 1** Crystal structure of complex **2a** (50 % probability ellipsoids). The DMSO molecules are omitted for clarity.

The 2 ligands were bonded to the Cd(II) in a meridional configuration with the 2 nitrogen atoms of the 2 ligands coordinating trans to each other, the 2 oxygen atoms and 2 sulfur atoms being cis to each other. The individual ligand bite angles [S12-Cd1-O2 144.96(6)°, S32-Cd1-O22 144.51(6)°] were similar to those seen in the related complexes [Cd(MIsDM)<sub>2</sub>] (145.61°), [Cd(MeIsChex)<sub>2</sub>] (143.8 and 145.0°), [Cd(Camp4Ph)<sub>2</sub>] (145.35 and 144.07°) and [Cd(SMeFur)<sub>2</sub>] 142.47 and 140.10° (MeIsDM = 1-(N-methylisatin)-4,4-dimethylthiosemicarbazonate, MeIsChex = 1-(N-methylisatin)-4-cyclohexylthiosemicarbazonate, (Camp4Ph)<sub>2</sub> = *RS*-camphor-4-phenylthiosemicarbazonate and SMeFur = *S*-methyl-(1-(furan-2-yl)ethylidene)dithiocarbazonate [27-30]). The bite angles within each ligand were smaller for N-Cd-O [70.19(8)° and 69.95(8)°] than for N-Cd-S [74.78(7)° and 74.56(7)°], all of which were comparable to those reported previously [27-30]. The C12-S12 and C32-S32 bond length increased

from 1.68 Å for **H1** [18] to 1.704(3) and 1.700(3) Å in the complex, confirming the coordination to the metal through the deprotonated thiolate form. Moreover, the shortening of the C12-N11 and C32-N31 bonds in the complex from 1.35 Å to 1.310(4) and 1.314(4) Å, compared to the free ligand, supporting the suggestion that the ligands coordinated with the Cd(II) ion in its enethiolate tautomeric form. Comparison of the cadmium coordinate bond lengths between **2a** and the related Cd(II) complexes containing 2 tridentate O-N-S<sub>thiolate</sub> ligands, [Cd(MeIsDM)<sub>2</sub>], [Cd(MeIsChex)<sub>2</sub>], [Cd(Camp4Ph)<sub>2</sub>] and [Cd(SMeFur)<sub>2</sub>] [27-30] shows these distances to be similar (**Table 2**).

**Table 2** Cd-donor atom distances (Å) of N-O-S<sub>thiolate</sub> tridentate six coordinate Cd(II) complexes.

Compound	Bond Type			Reference
	Cd-S	Cd-N	Cd-O	
2a	2.553(12)	2.321(3)	2.539(2)	This work
	2.566(12)	2.319(3)	2.523(3)	This work
[Cd(MIsDM) <sub>2</sub> ]	2.57	2.31	2.58	[27]
[Cd(MeIsChex) <sub>2</sub> ]	2.56, 2.57	2.30, 2.31	2.51, 2.52	[28]
[Cd(Camp4Ph) <sub>2</sub> ]	2.53, 2.55	2.31, 2.32	2.58, 2.63	[29]
[Cd(SMeFur) <sub>2</sub> ]	2.48, 2.50	2.29, 2.31	2.65, 2.71	[30]

#### Antibacterial activity

The antibacterial activity result of the assayed compounds is shown in **Table 3**. DMSO was employed as a negative control and did not exhibit any antibacterial activity, and the antibiotic streptomycin was screened as well for comparison. Schiff base **H1** was inactive against the 4 bacterial strains tested. In contrast, cadmium complex **2** exhibited significant antibacterial activity against the Gram positive *B. subtilis* (inhibition zone of 14 mm), comparable to the activity of streptomycin (inhibition zone of 15 mm). This observation however, could not provide evidence on the mode of action of complex **2** against *B. subtilis* as there are many other factors influencing the bactericidal activity of metal ions, including chelation, solubility, concentration, hydrophobicity, lipophilicity, geometry of the complex, coordinating sites and presence of co-ligands [31,32]. Indeed, chelation tends to enhance the bactericidal activity of **H1** as it exhibits more pronounced activity when coordinated to Cd<sup>2+</sup> ion. It is suggested that chelation causes a reduction in the polarity of the cadmium ion due to partial sharing of its positive charge with the ligand donor atoms and also because of delocalization of the  $\pi$  electron over the 4 chelate rings of complex **2**. These could then enhance the lipophilicity of compound, thus facilitating the interaction between Cd(II) metal ion with lipid membranes, which in turn leads to the disruption of the permeability barrier and prevent further growth of the bacteria [32].

**Table 3** Qualitative antibacterial assay.

Compound	Inhibitory activity (mm)			
	MRSA	<i>B. subtilis</i>	<i>P.aeruginosa</i>	<i>S.choleraesuis</i>
H1	–	–	–	–
2	–	14	–	–
DMSO	–	–	–	–
Streptomycin	25	15	20	17

(–) indicates the absence of inhibitory activity

## Conclusions

A new S-benzylthiocarbamate cadmium(II) complex containing 5-fluoroisatin ligand has been synthesized and characterized. Structural analysis showed that the ligands are monoanionic, coordinating in a doubly-chelating, tridentate manner, forming a 6-coordinate distorted octahedral complex. The Cd(II) complex manifests greater antibacterial activity compared to the free ligand, showing a similar level of inhibition to streptomycin against the Gram positive *B. subtilis*.

## Acknowledgements

Financial support is acknowledged from Universiti Teknologi MARA, Malaysia.

## References

- [1] Y Zhu, J Han, J Wang, N Shibata, M Sodeoka, VA Soloshonok, JA Coelho and FD Toste. Modern approaches for asymmetric construction of carbon-fluorine quaternary stereogenic centers: Synthetic challenges and pharmaceutical needs. *Chem. Rev.* 2018; **7**, 3887-964.
- [2] Y Ogawa, E Tokunaga, O Kobayashi, K Hirai and N Shibata. Current contributions of organofluorine compounds to the agrochemical industry. *iScience* 2020; **23**, 101467.
- [3] N Xu, J Shi, G Liu, X Yang, J Zheng, Z Zhang and Y Yang. Research progress of fluorine-containing electrolyte additives for lithium ion batteries. *J. Power Sources Adv.* 2021; **7**, 100043.
- [4] A Haider, L Gobbi, J Kretz, C Ullmer, A Brink, M Honer, TJ Woltering, D Muri, H Iding, M Bürkler, M Binder, C Bartelmus, I Knuesel, P Pacher, AM Herde, F Spinelli, H Ahmed, K Atz, C Keller, M Weber, R Schubli, L Mu, U Grether and SM Ametamey. Identification and preclinical development of a 2,5,6-trisubstituted fluorinated pyridine derivative as a radioligand for the positron emission tomography imaging of cannabinoid type 2 receptors. *J. Med. Chem.* 2020; **63**, 10287-306.
- [5] J Han, AM Remete, LS Dobson, L Kiss, K Izawa, H Moriwaki, VA Soloshonok and D O'Hagan. Next generation organofluorine containing blockbuster drugs. *J. Fluorine Chem.* 2020; **239**, 109639.
- [6] D O'Hagan. Understanding organofluorine chemistry. An introduction to the C-F Bond. *Chem. Soc. Rev.* 2008; **37**, 308-19.
- [7] MAFA Manan, DB Cordes, AMZ Slawin, M Bühl, VWY Liao, HC Chua, M Chebib and D O'Hagan. The synthesis and evaluation of fluoro-, trifluoromethyl-, and iodomuscimols as GABA agonists. *Chem. Eur. J.* 2017; **23**, 10848-52.
- [8] NA Meanwell. Fluorine and fluorinated motifs in the design and application of bioisosteres for drug design. *J. Med. Chem.* 2018; **61**, 5822-80.
- [9] Q Wu, JC Xiao, C Zhou, JR Sun, MF Huang, X Xu, T Li and H Tian. Crystal structure and supramolecular architecture of inorganic ligand-coordinated salen-type Schiff base complex: Insights into halogen bond from theoretical analysis and 3D energy framework calculations. *Crystals* 2020; **10**, 334.
- [10] P Basu, S Riyajuddin, TK Dey, A Ghosh, K Ghosh and SM Islam. Synthesis and architecture of polystyrene-supported Schiff base-palladium complex: Catalytic features and functions in diaryl urea preparation in conjunction with Suzuki-Miyaura cross-coupling reaction by reductive carbonylation. *J. Organomet. Chem.* 2018; **877**, 37-50.
- [11] X Liu, C Manzur, N Novoa, S Celedón, D Carrillo and JR Hamon. Multidentate unsymmetrically-substituted Schiff bases and their metal complexes: Synthesis, functional materials properties, and applications to catalysis. *Coord. Chem. Rev.* 2018; **357**, 144-72.
- [12] MAFA Manan, MIM Tahir, KA Crouse and FNF How. Distorted octahedral S-methyl(2-(2-oxoindolin-3-ylidene) hydrazinecarbodithioate (SMISA) tridentate Schiff base complex of Co(II): Synthesis, characterization and structural studies. *Malaysian J. Chem.* 2020; **22**, 25.
- [13] E Zangrando, MT Islam, MAAA Islam, MC Sheikh, MTH Tarafder, R Miyatake, R Zahan and MA Hossain. Synthesis, characterization and bio-activity of nickel (II) and copper (II) Complexes of a bidentate NS Schiff base of S-benzylthiocarbamate. *Inorg. Chim. Acta* 2015; **427**, 278-284.
- [14] A Hameed, M Al-Rashida, M Uroos, SA Ali and KM Khan. Schiff bases in medicinal chemistry: A patent review (2010 - 2015). *Expert Opin. Ther. Pat.* 2017; **27**, 63-79.
- [15] X Liu and Hamon JR. Recent developments in penta-, hexa-and heptadentate schiff base ligands and their metal complexes. *Coor. Chem. Rev.* 2019; **404**, 213109.
- [16] AZ El-Sonbati, WH Mahmoud, GG Mohamed, MA Diab, SM Morgan and SY Abbas. Synthesis, characterization of schiff base metal complexes and their biological investigation. *Appl. Organomet.*

- Chem.* 2019; **33**, e5048.
- [17] R Nath, S Pathania, G Grover and MJ Akhtar. Isatin containing heterocycles for different biological activities: Analysis of structure activity relationship. *J. Mol. Struct.* 2020; **1222**, 128900.
- [18] MAFA Manan, KA Crouse, MIM Tahir, R Rosli, FNF How, DJ Watkin and AMZ Slawin. Synthesis, characterization and cytotoxic activity of s-benzylthiocarbamate schiff bases derived from 5-fluoroisatin, 5-chloroisatin, 5-bromoisatin and their crystal structures. *J. Chem. Crystallogr.* 2011; **41**, 1630-41.
- [19] GM Sheldrick. *SAINT V4 software reference manual*. Siemens Analytical X-ray Systems, Madison, Wisconsin, 1996.
- [20] GM Sheldrick. *Program for empirical absorption correction of area detector data*. University of Göttingen, Göttingen, Germany, 1996.
- [21] MC Burla, R Caliendo, M Camalli, B Carrozzini, GL Cascarano, C Giacovazzo, M Mallamo, A Mazzone, G Polidori and R Spagna. R. SIR2011: A new package for crystal structure determination and refinement. *J. Appl. Crystallogr.* 2012; **45**, 357-61.
- [22] GM Sheldrick. Crystal structure refinement with SHELXL. *Acta Crystallogr. C* 2015; **71**, 3-8.
- [23] OV Dolomanov, LJ Bourhis, RJ Gildea, JAK Howard and H Puschmann. OLEX2: A complete structure solution, refinement and analysis program. *J. Appl. Crystallogr.* 2009; **42**, 339-41.
- [24] AW Bauer. Antibiotic susceptibility testing by a standardized single disk method. *Am. J. Clin. Pathol.* 1966; **45**, 493-6.
- [25] R Takjoo, R Centore and SS Hayatolghaibi. Mixed ligand complexes of cadmium (II) and copper (II) dithiocarbamate: Synthesis, spectral characterization, x-ray crystal structure. *Inorg. Chim. Acta.* 2018; **471**, 587-94.
- [26] A Banerjee, M Mohanty, S Lima, R Samanta, E Garribba, T Sasamori and R Dinda. Synthesis, structure and characterization of new dithiocarbamate-based mixed ligand oxidovanadium(IV) complexes: DNA/HSA interaction, cytotoxic activity and DFT studies. *New J. Chem.* 2020; **44**, 10946-63.
- [27] E Labisbal, A Sousa-Pedrares, W Kaminsky and DX West. Structure of N-methylisatin N(4)-dimethylthiosemicarbazone and its electrochemically synthesized 6-coordinate cadmium(II) complex. *Z. Naturforsch. B* 2002; **57**, 908-13.
- [28] E Labisbal, A Sousa, A Castiñeiras, JA García-Vázquez, J Romero, GA Bain and DX West. Electrochemical synthesis of a 6-coordinate cadmium(II) complex with N-methylisatin N(4)-cyclohexylthiosemicarbazone. *Zeitschrift für Naturforschung B* 2000; **55**, 162-6.
- [29] VS Nogueira, L Bresolin, C Näther, I Jess and ABD Oliveira. Crystal structure of cis-bis-[4-phenyl-1-[(3R)-1,7,7-tri-methyl-2-oxobicyclo-[2.2.1]heptan-3-ylidene]thiosemicarbazidato  $\kappa^3\text{O},\text{N}^1,\text{S}$ ]=cadmium(II) with an unknown solvent molecule. *Acta Crystallogr. Sect. E.* 2015; **71**, m234 - m235.
- [30] KB Chew, MTH Tarafder, KA Crouse, AM Ali, BM Yamin and HK Fun. Synthesis, characterization and bio-activity of metal complexes of bidentate N-S isomeric Schiff bases derived from S-methylthiocarbamate (SMDTC) and the X-ray structure of the bis[S-methyl- $\beta$ -N-(2-furylmethylketone)dithiocarbazato]cadmium(II) complex. *Polyhedron* 2004; **23**, 1385-92.
- [31] ZH Chohan, A Munawar and Ct Supuran. Transition metal ion complexes of schiff-bases. Synthesis, characterization and antibacterial properties. *Met. Based Drug.* 2001; **8**, 137-143.
- [32] MA Malik, OA Dar, P Gull, MY Wani and AA Hashmi. Heterocyclic Schiff base transition metal complexes in antimicrobial and anticancer chemotherapy. *MedChemComm.* 2018; **9**, 409-436.